Regular Article

PHYSICAL CHEMISTRY RESEARCH
Published by the
Iranian Chemical Society
www.physchemres.org
info@physchemres.org

Phys. Chem. Res., Vol. 11, No. 3, 643-651, September 2023
DOI: 10.22036/pcr.2022.352163.2139

Quantum Calculations of some Electronic and Structural Parameters for the System of Vitamin C and Different Sulfoxide Solvents

N. Niazazari and M.R. Toosi*

Department of Chemistry, Qaemshahr Branch, Islamic Azad University, Qaemshahr, Iran

(Received 18 July 2022, Accepted 27 September 2022)

DFT modeling was applied to determine the structural and electronic properties of L-ascorbic acid (AA) in three homologous sulfoxides as solvents (dimethyl, diethyl, and dipropyl sulfoxide) using 6-31++G** basis set and B3LYP level. NBO analysis was used to evaluate Mulliken charge, electron donor and electron acceptor in AA/DRSO system. Vibrational analysis was evaluated in order to estimate normal frequencies and characteristics of hydrogen bonds formed due to the interactions between hydroxyl groups of AA and sulfoxide in the solvent. Our results showed that DFT/B3LYP method with 6-31++G** basis set is a good candidate method for quantum calculation of AA/DRSO systems. It was found that the geometrical and electronic properties such as the bond length and Mulliken charge remarkably changed after the formation of hydrogen bonds between oxygen of S=O group in sulfoxide and hydroxyl groups located on lactan ring. Charge analysis indicated that the positive charge of sulfur atom decreased by an increase of alkyl groups in the solvent. Charge transfer (Δq) and polarity of the S=O bond in DESO were higher than those in other solvents. Vibrational analysis showed that the strongest hydrogen bond was formed in the AA/DESO system.

Keywords: Ascorbic acid, DFT, Biological compound, B3LYP, Hydrogen bond, Vibrational frequency

INTRODUCTION

Structure of biological/biochemical compounds in the presence of organic solvents during synthesis of pharmaceutical compounds is important in biochemical reactions. In addition, study of the nature of interactions between biomolecules and organic solvents provides useful information about their activities or properties during the process of drug synthesis. Several properties of these compounds such as chemical stability, reactivity, nucleophilicity, electrophilicity, acidity, solubility and biological factors (*i.e.* target activity and biotransformation ability in biological systems) can be affected in the presence of organic solvents. On the other hand, chemical nature of organic solvent and chemical properties such as polarity, type of functional group, and presence or absence of labile proton (protic/aprotic) in solvent structure play key roles in different conditions during organic reactions.

DFT modeling is a useful method for studying the characteristics of biomolecules/solvent systems according to the detailed information of DFT calculations about structural and electronic properties. DFT calculations have been widely used for the several systems of biological or pharmaceutical compounds in different solvents such as Ferulic acid/water, ethanol, DMSO [1], 3-hydroxyflavone/DMSO [2], azo Schiff base/polar solvents [3], benzimidazoles/DMSO or CH_3Cl [4], 2-methylpyridine 1-oxide/DMSO or CH_3Cl [5], vitamin K_3 [6], *etc*.

L-ascorbic acid (AA; vitamin C) as an important antioxidant reagent plays a key role in the enzymatic reactions by donating electrons and scavenging reactive oxygen species (ROS), which are by-products of normal cell metabolism [7]. Its antioxidant activity can be extremely affected by the factors that can change stability of the ionized

*Corresponding author. E-mail: mrtoosi@gmail.com

(ascorbate) or non-ionized (ascorbic) form acting as reducing agent in biological reactions. Another interesting application of AA is its usage as a substrate for synthesis of organic compounds in-vitro, especially for the synthesis of optically active natural products [8]. It is used to produce chiral drugs such as aryloxypropanolamines (β-blockers), γ-Amino-β-hydroxybutyric acid, GABOB (anticonvulsant), L-threonolactone [9], and 3-hexulose [10]. Several food additives which are generally used as antioxidant are synthesized using AA as precursor, such as ascorbyl palmitate (formed by reaction between ascorbic acid and palmitic acid) or ascorbyl stearate as an ester of both ascorbic and stearic acids. So, it is important to understand solvent effect on the properties of AA in organic synthesis. Antioxidant activity of AA was modeled by DFT calculations via trapping methyl peroxyl radicals at the presence of the solvents with different polarities [11]. DFT calculations were also used for modeling the optimized structures of the transition states of AA in water [12] and to further study of the variation of the vibrational frequencies of different AA conformations in DMSO [13] and water [14].

Another application of computational modeling is vibrational studies and other spectral analyses of the biomolecules in individual form or in the presence of the solvent. DFT modeling and NBO analysis can be used for FTIR and FT Raman spectra, NMR, and UV spectroscopy of the chemical or biological compounds [15-18]. Sometimes, it is important to find out the relationship between the chemical structures and the molecular spectroscopy of the compounds using QSAR [19]. The structural and vibrational analysis of benzil and its halogenated analogues were performed by QSAR method in order to investigate relationship between the experimental data and calculated Raman and IR frequencies [20]. QSAR method was also used to study the surface activity of imidazoline and its derivatives, commonly used as surfactant, emulsifier, corrosion inhibitor, *etc*. [21]. The results showed good correlation between predicted data and experiments. Vibrational analysis and its structure relationship were studied for 4-hydroxybenzamide as an important antifungal or antimicrobial reagent used in medical and pharmaceutical industries [22]. Similar calculation and comparison with the experimental data were applied for the 3-amino-3-(2-nitrophenyl) propionic acid [23] and 2-hydroxybenzhydrazied [24].

In the present study, we have modeled AA molecule in three homologues sulfoxide solvents using DFT calculations. We have studied geometrical parameters and electronic properties of AA/solvent systems and also investigated the qualitative correlation between the molecular properties of the system and the solvent structure.

COMPUTATIONAL DETAILS

We selected three types of dialkyl sulfoxide including methyl, ethyl, and propyl groups (DMSO, DESO, DPSO, respectively) that are usually liquid in ambient temperature; hence, they can interact with the biological compounds as polar aprotic solvent in liquid medium. The optimization of AA structure and geometrical parameters were initially performed by Hyperchem 6.0 software [25] using semi-empirical molecular orbital theory (AM1 method) shown in Fig. 1 (The additional atoms of C and H are neglected in DMSO or DESO). Afterwards, quantum calculations for the optimized structure of AA/DRSO system (R = Me, Et, or Pr) were done by DFT method using Gaussian 98 package [26] and 6-31++G** basis set at B3LYP level.

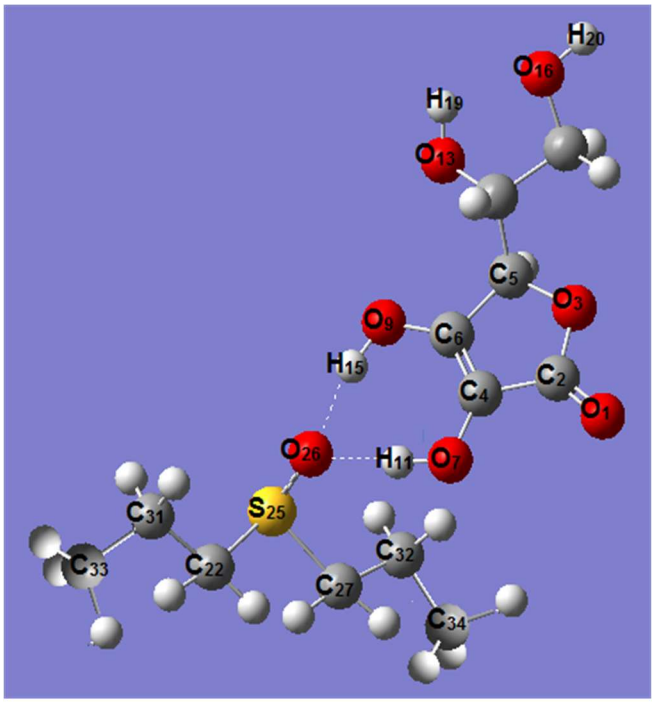

Fig. 1. The optimized structure of AA/DRSO system.

In order to study of the solvent effect on the optimum configurations of AA/DRSO systems in comparison to the gas phase, Onsager method was applied as the continuum solvation model for AA in each solvent using corresponding dielectric constant (46.68, 44.82, and 31.10 for DMSO, DESO, and DPSO, respectively). NBO analysis was used to estimate Mulliken charge, electron donor, and electron acceptor in AA/DRSO system. Vibrational analysis was evaluated by Gaussview package [27] for the frequencies of intramolecular bonds and hydrogen bonds formed between hydroxyl groups of AA and sulfoxide group in each solvent. Simulation of UV-Vis spectra of AA/DRSO was carried out using B3LYP functional and 6-31++G** basis set.

Energy calculations were obtained by evaluating the difference between the energy values of AA/solvent system and that of individual molecules using basis set super position error, using the following equation:

$$E_{int} = E_{L\text{-}AA/DESO} - E_{L\text{-}AA} - E_{DESO} + E_{BSSE}$$

Dipole moment and its variation during the interaction were also estimated for determining variation in the polarity of the systems before and after h-bond formation. FT-IR and Raman spectra of AA/DRSO mixtures were performed using Thermo instrument (AVATAR, USA) in the range of 400-4000 cm^{-1} and by the resolution of 2 cm^{-1} (for FTIR) and Teksan device (P50C0R10) using a laser power 200 mW at λ = 1064 nm and resolution of 2 cm^{-1} equipped with a thermostatic cell holder at a sample temperature of 25 °C (for Raman).

RESULTS AND DISCUSSION

Table 1 shows main geometrical parameters of the three AA/DRSO (R: methyl, ethyl, propyl) complexes in gas and

Table 1. Main Geometrical Parameters of Three AA/DRSO (R: Methyl, Ethyl, Propyl) Complexes in Gas and Liquid Phase (Distance Unit: Angstrom; Angle Unit: Degree)

Parameter	Exp. [14]	Theo. [28]	Gas phase			SCRF		
			DMSO	DESO	DPSO	DMSO	DESO	DPSO
C_2=O_1	1.216	1.211	1.206	1.202	1.208	1.215	1.212	1.210
C_4=C_6	1.338	1.343	1.350	1.351	1.355	1.360	1.358	1.355
C_5-O_3	1.444	1.450	1.438	1.434	1.441	1.440	1.437	1.437
C_2-O_3	1.355	1.377	1.386	1.383	1.387	1.395	1.397	1.394
C_6-O_9	1.326	1.347	1.355	1.338	1.341	1.337	1.336	1.341
C_4-O_7	1.361	1.358	1.356	1.354	1.359	1.347	1.351	1.351
O_9-H_{15}	NA	NA	0.992	0.980	0.986	1.013	1.027	1.014
O_7-H_{11}	NA	NA	0.978	0.977	0.982	0.992	0.984	0.984
O_{26}…H_{15}	NA	NA	1.701	1.796	1.751	1.584	1.528	1.589
O_{26}…H_{11}	NA	NA	1.846	1.796	1.771	1.748	1.831	1.857
C_2-C_4	1.452	1.457	1.465	1.465	1.465	1.472	1.465	1.468
C_5-C_6	1.493	1.501	1.508	1.507	1.508	1.499	1.504	1.504
O_{16}-H_{20}	NA	NA	0.968	0.962	0.964	0.943	0.970	0.975
O_{13}-H_{19}	NA	NA	0.973	0.966	0.969	0.943	0.973	0.972
S_{25}-C_{27}	NA	NA	1.825	1.830	1.843	1.793	1.836	1.840
S_{25}-C_{22}	NA	NA	1.829	1.830	1.840	1.792	1.836	1.834
C_{27}-C_{32}	NA	NA	-	1.528	1.532	-	1.526	1.531
C_{22}-C_{31}	NA	NA	-	1.527	1.531	-	1.526	1.530
S_{25}=O_{26}	NA	NA	1.549	1.525	1.553	1.573	1.576	1.571
< O_9-H_{15}…O_{26}	NA	NA	169.363	168.958	168.248	164.127	168.368	168.269
< O_7-H_{11}…O_{26}	NA	NA	161.169	167.992	167.738	162.241	160.212	162.288
< C_{27}-S_{25}-C_{22}	NA	NA	98.613	98.191	98.138	99.100	98.938	98.622

liquid phase. In order to validate quantum calculations for the optimized structures, the computational results for several bond lengths of AA (geometrical parameters) were compared with the experimental data [14] and shown in Fig. 2. A reasonable correlation was obtained between computational results and the experiment (values of R^2 are 0.964, 0.965, and 0.968 for DMSO, DESO, and DPSO, respectively). So, it can be concluded that 6-31++G** basis set and DFT/B3LYP method are suitable to evaluate the structural and electronic properties of the AA/DRSO systems.

Figure 3 shows geometrical parameters of AA/DRSO systems. It was obtained that by variation of the alkyl group, the bond lengths locating far from the h-bonds do not change significantly. However, the alkyl group affects the bond distances of hydrogen bonds (*i.e.* $O_{26}…H_{11}$ and $O_{26}…H_{15}$) as the main interaction sites between the two molecules. For the case of $O_{26}…H_{11}$, the bond length increased by variation of the alkyl group, from 1.748 Å for methyl to 1.857 Å for propyl. Variations in $O_{26}…H_{15}$ bond lengths were 1.584, 1.528, and 1.589 Å for methyl, ethyl, and propyl, respectively. It was obtained that the bond length of $O_{26}…H_{15}$ was smaller than $O_{26}…H_{11}$ exhibiting a minimum value for the ethyl group. The second significant variation belonged to the O_{13}-H_{19} with values of 0.943, 0.97, and 0.975 Å, and also O_{16}-H_{20} with values of 0.943, 0.973, and 0.972 Å for DMSO, DESO, and DPSO, respectively. The third remarkable change was obtained in the bond length of S_{25}-C_{27} and S_{25}-C_{22}. The bond lengths of S_{25}-C_{27} were 1.793, 1.836, and 1.840 Å for DPSO, DESO, and DPSO, respectively. These values for S_{25}-C_{27} bond were 1.792, 1.836, and 1.834 Å, respectively. This is due to electron donating property of alkyl groups that obey the trend Me > Et > Pr, leading to a decrease in electron affinity of the sulfur atom and difference of electronegativity between S and C atoms, which further results in an increase in the bond length.

The total energy values for AA/DRSO were -3250582 × 10^5, -3457034 × 10^5, and -3663471 × 10^5 kJ mol^{-1}, respectively. The values of ΔE were -123.47, -189.41, and -110.00 kJ mol^{-1}, respectively. In addition, according to the DFT calculations, dipole moments of AA/DRSO systems were 21.9372, 21.3146, and 19.8292 Debye and Δμ's (Δμ = μ complex - Σμ free molecules) were 10.594, 14.0085, and 12.6291 Debye, respectively. Comparison of the Δμ values for the liquid and gas phase (not shown here) showed that the

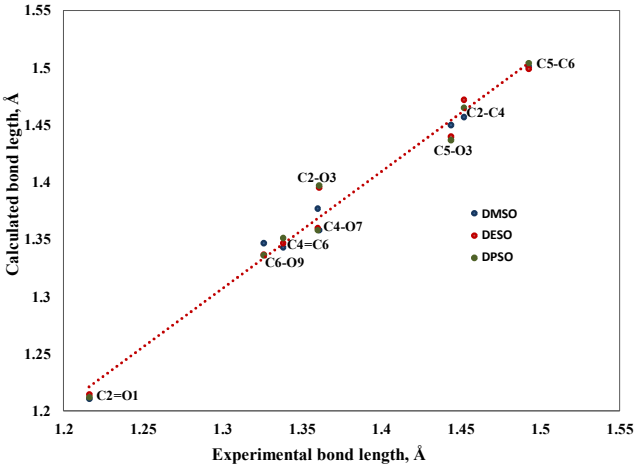

Fig. 2. Correlation curve of theoretical bond length vs. experimental data [14].

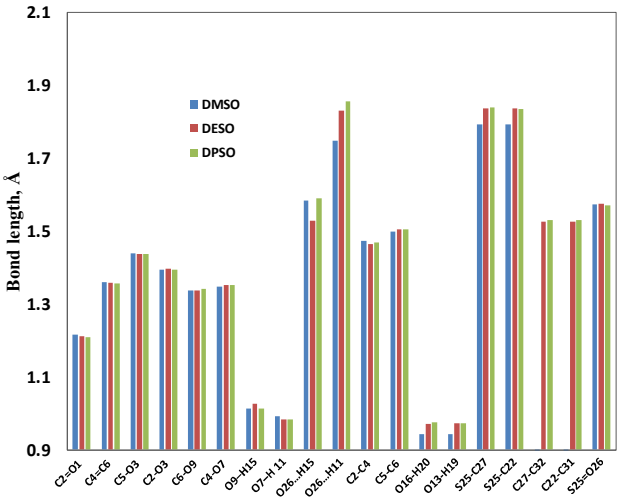

Fig. 3. values of bond length for main sites of AA/DRSO system.

stability of AA molecules in the presence of the solvent was more than that for individual molecules. Both values of ΔE and Δμ had a maximum value for DESO.

Details of NBO analysis for the region of interaction between AA and DRSO are shown in Table 2. In the below formulation, E(2) is the energy of hyper conjugative interaction (stabilization energy):

$$E(2) = q_i (F_{ij}^2/E_j - E_i)$$

Table 2. Results of NBO Analysis for L-AA/DRSO (R: Methyl, Ethyl, Propyl) Complexes

Solvent	Donor NBO	Acceptor NBO	E_g (eV)	E(2) (eV)
DMSO	O_7	S_{25}-C_{22}	4.306	0.0312
	O_9	S_{25}-C_{22}	4.306	0.0372
DESO	O_7	S_{25}-O_{26}	4.313	0.0095
	O_9	S_{25}-O_{26}	4.313	0.0087
DPSO	O_{26}	S_{25}-C_{22}	4.08	0.0385
	O_{26}	S_{25}-C_{22}	4.07	0.0436

Here, q_i is the orbital occupancy, E_i, E_j are diagonal elements, and $F_{i,j}$ is the off-diagonal element of NBO Fock matrix. The results showed that the lone pair (LP) orbitals of oxygen of hydroxyl groups in AA (O_7 and O_9) acted as electron donor in DMSO and DESO while the LP orbital of oxygen in sulfoxide group (O_{26}) was electron donor. In addition, the lone vacant (LV) orbital of sulfur in S-C bond was the electron acceptor in AA/DMSO and AA/DPSO systems, and S=O bond acts as an electron acceptor in DESO. Maximum value of E(2) during electron density transfer between LP donor and LV acceptor was 0.0436 eV in AA/DPSO system. Experimental results for UV absorption spectrum of AA showed the main absorption band at 263 nm [29]. Our modeling calculated this band at 271.6 nm for AA alone. This band was calculated as 272.1, 273.8, and 273.1 nm for the solution of AA in DMSO, DESO, and DRSO, respectively. As the sulfoxide solvents have not any absorption in UV-Vis spectrometer, it can be concluded that the interaction of AA with the sulfoxide solvents does not have any absorption in UV-Vis range and cannot significantly change the UV absorption band of AA.

Mulliken charges for the S=O in the solvent and O-H group of AA in the AA/DRSO systems are shown in Fig. 4. It was obtained that the positive charge on sulfur decreased by an increase in alkyl group of the solvent. For the oxygen of S=O group of the solvent, maximum negative charge was -0.9846 e^- for DESO. It can be concluded that the polarity of the S=O bond in DESO was higher than the others. The charge value of O_9 in AA did not change significantly, but the value for another one (O_7) reached to a maximum value (-0.6418 e^-) in DESO. The charge transfers (absolute value of difference between charges of positive and negative sites;

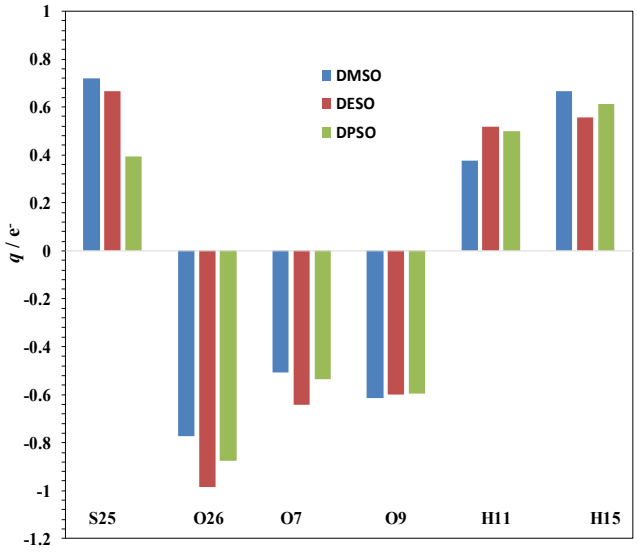

Fig. 4. Charge values for sulfur, oxygen and hydrogen atoms of S=O...H-O system in AA/DRSO complex.

Δq|) for O_{26}…H_{11} were 1.147, 1.502, and 1.373 e^- for DMSO, DESO, and DPESO, respectively. |Δq|'s for the O_{26}…H_{15} bond were 1.436, 1.539, and 1.488 e^-, respectively. This means that the polarity of h-bond in DESO was higher than that in the other solvents. This was confirmed by the higher values of ΔE and Δμ in AA/DESO system.

Table 3 shows some vibrational frequencies of AA/DRSO systems. According to the results, the strongest h-bond was formed in the AA/DESO system. According to Fig. 4, the higher negative charge of oxygen in S=O group of DESO had higher tendency toward the hydrogens of O-H groups in ascorbic acid. Detailed analysis of frequencies for

Table 3. Selected FTIR Vibrational Frequencies of the Complexes in Liquid Phase at DFT/6- 31++G** Level

Frequencies (υ)	Experimental (cm^{-1})	Calculated frequencies (cm^{-1})		
		DMSO	DESO	DPSO
$(O_{26}…H_{11})^a$	1079, 1134, 1043	365.784	955.70	734.980
$(O_{26}…H_{15})^a$	1160, 1204, 1148	845.124	1012.55	963.468
S_{25}-C_{27}	669	643.80	631.48	689.02
S_{25}-C_{22}	669	646.819	646.01	697.313
C_{27}-C_{32}	1489	1091.34	971.46	846.261
C_{22}-C_{31}	1489	1093.52	979.22	897.313
C_6-O_9	1131	1334.24	1209.78	1057.54
C_4-O_7	1131	1091.46	1320.29	1337.71
C_2-C_4	826	1223.19	1364.11	1337.71
C_5-C_6	826	1215.06	1359.74	1340.68
C_2-O_3	1131	1091.46	991.86	736.255
C_5-O_3	1131	1047.74	1045.72	736.255
C_2=O_1	1761	1722.66	1841.85	1843.74
C_4=C_6	1693	1615.19	1720.29	1726.45
S_{25}=O_{26} [a]	1025, 1057, 1069	1626.34	991.863	963.468
O_9-H_{15}	3304	2603.02	3483.54	3418.49
O_7-H_{11}	3304	2950.49	3547.43	3515.88
O_{16}-H_{20}	3304	3384.87	3859.90	3853.02
O_{13}-H_{19}	3304	3376.40	3785.49	3784.65

[a]Experimental values were observed for DMSO, DESO, and DPSO, respectively.

the various bonds in AA structure showed that the strength of C-C bonds decreased by an increase of alkyl group in the solvent. Variation in strength of the bonds between carbon and hydroxyl group (C_6-O_9 and C_4-O_7) was complicated, but the strength of C-O bonds in lactan ring decreased by an increase in the molecular size of the solvent. The frequency of carbonyl bond was increased by an increase in alkyl group in the solvent. This behavior was disappeared for C=C bond of lactan ring. Finally, the strongest O-H bond was disappeared in the AA/DESO system.

Comparison of the frequencies for S-C bonds showed that the strongest bond was disappeared in the AA/DPSO system. In addition, it was obtained that the strength of the S=O band decreased by the increase of alkyl group in the solvent. Considering the effect of bond length on the value of vibrational frequency, it was found that there was not a significant relationship between the bond length and frequency. For example, the frequency decreased by an increase in the bond length of C_5-O_3 bonds; however, the frequency decreased by an increase in the bond length of C_6-O_9. Among the hydroxyl groups, increase in the bond length of O_{13}-O_{19} and O_{16}-H_{20} bonds led to an increase in the vibrational frequency; for O_9-H_{15} and O_7-H_{11} there was not a significant behavior. Increase in the frequency was also obtained by an increase in the bond lengths of C=C and S-C bonds. To compare the calculated results of vibrational frequencies with the experimental results, FTIR spectra of the three mixtures of AA and DRSO mixtures are shown in Fig. 5.

Table 4 shows the main vibrational bands in Raman spectra of AA/DRSO mixtures. Experimental results demonstrate eight peaks in the Raman spectra. Comparison of the details for pure AA and the solvents [9] shows an increase of the frequencies which can be related to the increase in the polarizibilty of AA/DRSO mixture.

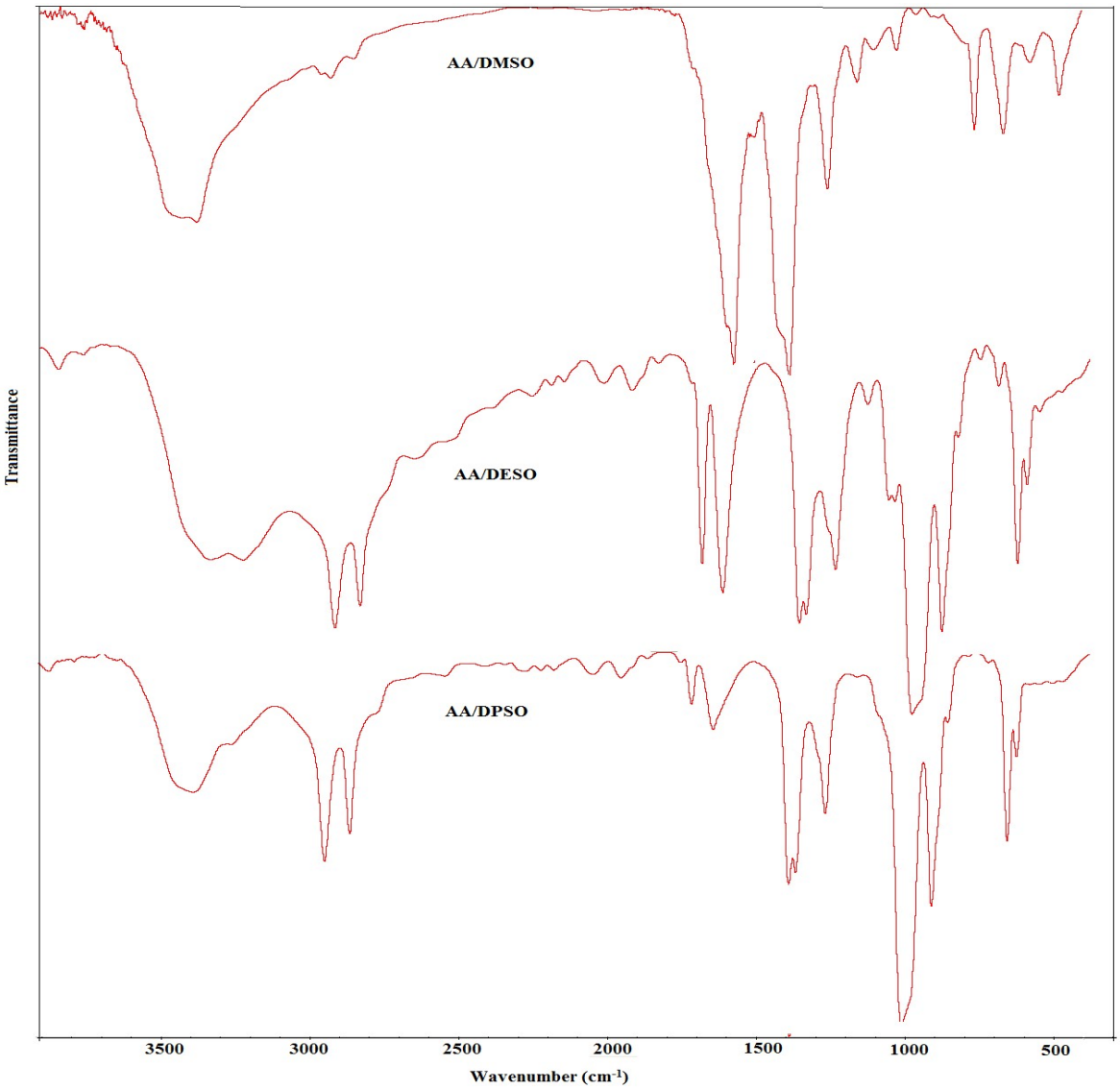

Fig. 5. FTIR spectra of three solutions of AA different solvents (0.5 M).

Table 4. Selected Observed Raman Vibrational Frequencies of AA/DRSO

Frequencies (υ)	Experimental	Calculated frequencies (cm^{-1})		
		Solvent		
		DMSO	DESO	DPSO
C_{AA}-H_{AA}	3002	3287.50	3302.39	3250.07
C_{22}-C_{31}	1489	1519.90	1541.55	1505.34
C_6-O_9	1105	1170.48	1191.59	1163.88
C_2=O_1	1764	1783.41	1790.66	1765.02
C_4=C_6	1414	1444.07	1458.90	1432.19
S_{25}=O_{26}	1026	1088.27	1075.68	1072.04
C_5-C_6	871	1003.04	1029.27	1010.96
C_S-H_S	2920	3007.71	3025.11	30016.02

CONCLUSIONS

Our calculations showed that DFT/B3LYP method with 6-31++G** basis set is good candidate method for quantum calculation of AA/DRSO systems. It was found that the most changes in the bond lengths were due to interaction between AA and the solvent, especially hydrogen bond formation between the oxygen of S=O group of sulfoxide solvent and hydroxyl groups located on lactan ring. Charge analysis indicated that the positive charge of sulfur decreased by the increase of alkyl groups. Charge transfer (Δq) and polarity of S=O bond in DESO were higher than those in the other solvents. Vibrational analysis showed that the strongest hydrogen bond was formed in the AA/DESO system.

ACKNOWLEDGEMENTS

This work was supported by Qaemshahr Branch of Islamic Azed University (IAU) and the corresponding author (M. R. Toosi) received research support from Takin Shimi Company. The co-author (N. Niazazari) declares he has no financial interests.

REFERENCES

[1] Urbaniak, A.; Szelag, M.; Molski, M. Theoretical investigation of stereochemistry and solvent influence on antioxidant activity of ferulic acid. *Comput. Theor. Chem.* **2013**, *1012*, 33, DOI: 10.1016/ j.comptc.2013.02.018.

[2] Protti, S.; Mezzetti, A.; Cornard, J. -P.; Lapouge, C.; Fagnoni, M., Hydrogen bonding properties of DMSO in ground-state formation and optical spectra of 3-hydroxyflavone anion. *Chem. Phys. Let.* **2008**, 467, *88*, DOI: 10.1016/j.cplett.2008.11.005.

[3] Gözel, A; Kose, K.; Karakas, D.; Atabey, H.; McKee, V.; Kurtoglu, M., pectral, structural and quantum chemical computational and dissociation constant studies of a novel azo-enamine tautomer. *J. Mol. Struct.* **2014**, *1074*, 449, DOI: 10.1016/j.molstruc.2014.06.033.

[4] Abdel Ghani, N. T.; Mansour, A. M., Molecular structures of 2-arylaminomethyl-1H-benzimidazole: Spectral, electrochemical, DFT and biological studies. *Spectrochim. Acta A* **2012**, *91*, 272, DOI: 10.1016/j.saa.2012.01.080.

[5] Shoba, D.; Periandi, S.; Boomadevi, S.; Ramalingam, S.; Fereyduni, E. FT-IR, FT-Raman, UV, NMR spectra, molecular structure, ESP, NBO and HOMO-LUMO investigation of 2-methylpyridine 1-oxide: A combined experimental and DFT study. *Spectrochim. Acta A: Mol. Biomol. Spect.* **2014**, *118*, 438, DOI: 10.1016/j.saa.2013.09.023.

[6] Khaikin, L. S.; Tikhonov, D. S.; Grikina, O. E.; Rykov, A. N.; Stepanov, N. F., Radical scavenging activity of ascorbic acid analogs: kinetics and mechanisms. *Russ. J. Phys. Chem.* **2014**, *88*, 886, DOI: 10.1134/S0036024414050112.

[7] Muthu, S.; Isac Paulraj, E., Molecular structure, vibrational spectra, first order hyper polarizability, NBO and HOMO-LUMO analysis of 4-amino-3(4-chlorophenyl) butanoic acid. *Solid State Sci.* **2012**, *14*, 476-487, DOI: 10.1016/ j.solidstatesciences.2012.01.028.

[8] Jung, M. E.; Shaw, T. J., Total Synthesis of (R)-Glycerol Acetonide and the Antiepileptic and Hypotensive Drug (-)-y-Amino-P-hydroxybutyric Acid (GABOB): Use of Vitamin C as a Chiral Starting Material. *J. Am. Chem. Soc.* **1980**, *102*, 6304-6311, DOI: 10.1021/ ja00540a022.

[9] Tadao, K.; Noriko, M.; Yuzuru, O., Formation of L-Threonolactone and Oxalic Acid in the Autoxidation Reaction of L-Ascorbic Acid: Possible Involvement of Singlet Oxygen. *Biosci., Biotech., and Biochemistry* **1996**, *60*, 1212-1214, DOI: 10.1271/bbb.60.1212.

[10] Kim, K. S.; Lee, H. S.; Kim, S. C.; Hahn, C. S., Synthesis of Allyl Ether Derivatives of L-Ascorbic Acid, *Bulletin of Korean Chem. Soc.*, **1984**, Vol. 5t, 6.

[11] Ardjani, T. E. A.; Alvarez‐Idaboy, J. R., Radical scavenging activity of ascorbic acid analogs: kinetics and mechanisms *Theor. Chem. Accounts* **2018**, *137*, 69, DOI: 10.1007/s00214-018-2252-x.

[12] Demianenko, E.; Ilchenko, M.; Grebenyuk, A.; Lobanov, V.; Tsendra, O., A theoretical study on ascorbic acid dissociation in water clusters. *J. Mol. Model.* **2014**, *20*, 2128, DOI: 10.1007/s00894-014-2128-5.

[13] Niazazari, N.; Zatikyan, A. L.; Markarian, S. A., *Ab initio* and DFT study of hydrogen bond interactions

between ascorbic acid and dimethylsulfoxide based on FT-IR and FT-Raman spectra. *Spectrochim. Acta A Mol. Biomol. Spect.* **2013**, *110*, 217, DOI: 10.1016/j.saa.2013.03.029.

[14] Bichara, L. C.; Lanus, H. E.; Nieto, C. G.; Brandan, S. A., Density Functional Theory Study of Catechol Adhesion on Silica Surfaces. *J. Phys. Chem. A* **2010**, *114*, 4997, DOI: 10.1021/jp1070538.

[15] Aayisha, S.; Renuga, Devi, T. S.; Janani, S.; Muthu, S.; Raja, M.; Sevvanthi, S., DFT, molecular docking and experimental FT-IR, FT-Raman, NMR inquisitions on "4-chloro-N-(4,5-dihydro-1H-imidazol-2-yl)-6-methoxy-2-methylpyrimidin-5-amine": Alpha-2-imidazoline receptor agonist antihypertensive agent, *J. Mol. Struct.* **2019**, *1186*, 468-481, DOI: 10.1016/j.molstruc.2019.03.056.

[16] Kuruvilla, T. K.; Muthu, S.; Prasana, J. C.; George, J.; Sevvanthi, S., Spectroscopic (FT-IR, FT-Raman), quantum mechanical and docking studies on methyl[(3S)-3-(naphthalen-1-yloxy)-3-(thiophen-2-yl)propyl]amine. *J. Mol. Struct.* **2019**, *1175*, 163-174, DOI: 10.1016/j.molstruc.2018.07.097.

[17] Muthu, S.; Porchelvi, E. E.; Karabacak, M.; Asiri, A. M.; Swathi, S. S., Synthesis, structure, spectroscopic studies (FT-IR, FT-Raman and UV), normal coordinate, NBO and NLO analysis of salicylaldehyde p-chlorophenylthiosemicarbazone, *J. Mol. Struct.*, **2015**, *1081*, 400-412, DOI: 10.1016/j.molstruc.2014.10.024.

[18] Muthu, S.; Aayisha, S.; Suresh, M.; Thamarai, A.; Raj Muhamed, R.; Raja, M., Synthesis, spectroscopic elucidation (FT-IR, FT-Raman, UV-Vis), electronic properties and biological activities (antimicrobial, docking) of semicarbazide derivative. *Mater. Today: Proceedings*, **2022**, *50*, 2847-2852, DOI: 10.1016/j.matpr.2020.09.569.

[19] Amiri, M.; Fazli, M.; Ajloo, D., QSAR, Docking and Molecular Dynamics Studies on the Piperidone-grafted Mono- and Bis-spiro-oxindole-hexahydropyrrolizines as Potent Butyrylcholinesterase Inhibitors. *Phys. Chem. Res.* **2018**, *6*, 685-711, DOI: 10.22036/pcr.2018.109597.1438.

[20] Shyma Mary, Y.; Sheena Mary, Y.; Resmi, K. S.; Kumar, V. S.; Thomas, R.; Sureshkumar, B., Detailed quantum mechanical, molecular docking, QSAR prediction, photovoltaic light harvesting efficiency analysis of benzil and its halogenated analogues. *Heliyon* **2019**, *5*, e02825, DOI: 10.1016/j.heliyon.2019.e02825.

[21] Kong, X.; Qian, C.; Fan, W.; Liang, Z., Experimental and QSAR study on the surface activities of alkyl imidazoline surfactants. *J. Mol. Struc.* **2018**, 1156, *164*, DOI: 10.1016/j.molstruc.2017.11.102.

[22] Ramesh, P.; Lydia Caroline, M.; Muthu, S.; Raja, M.; Geoffrey, A. S. B.; Aayisha, S.; David, H. A., Theoretical and experimental spectroscopic studies of monomeric and dimeric structures of 4-hydroxybenzamide. *J. Mol. Struc.* **2020**, *1206*, 127742, DOI: 10.1016/j.molstruc.2020.127742.

[23] Abraham, C. S.; Muthu, S.; Prasana, J. C.; Rizwana, B. F.; Armaković, S.; Armaković, S. J., Vibrational and electronic absorption spectroscopic profiling, natural hybrid orbital, charge transfer, electron localization function and molecular docking analysis on 3-amino-3-(2-nitrophenyl) propionic acid. *J. Mol. Struc.* **2018**, *1171*, 733, DOI: 10.1016/j.molstruc.2018.06.057.

[24] Ramesh, P.; Lydia Caroline, M.; Muthu, S.; Thamarai, A.; Raja, M.; Aayisha, S.; Antony David, H., Spectroscopic (FT-IR, FT-Raman) investigations, chemical properties, antimicrobial and molecular docking analyses of 2-hydroxybenzhydrazied *Mater. Today*: Proceedings **2022**, *50*, 2640, DOI: 10.1016/j.matpr.2020.07.592.

[25] http://www.hypercubeusa.com/?tabid=360

[26] https://gaussian.com/

[27] https://gaussian.com/gaussview6/

[28] Panicker, C. Y.; Varghese, H. T.; Philip, D., FT-IR, FT-Raman and SERS spectra of Vitamin C. *Spectrochim. Acta A,* **2006**, *65*, 802, DOI: 10.1016/j.saa.2005.12.044.

[29] Singh, G.; Mohanty, B. P.; Saini, G. S. S., Structure, spectra and antioxidant action of ascorbic acid studied by density functional theory, Raman spectroscopic and nuclear magnetic resonance techniques, *Spectrochim. Acta - A: Mol. Biomol*. **2016**, *155*, 61, DOI: 10.1016/j.saa.2015.11.005.